

## Heterogeneous Nucleation Effect of *N, N'*-Adipic Bis(4-phenylbutyric Acid) Dihydrazide on Crystallization Process of Poly(L-lactic Acid)

Yanhua CAI\*, Lisha ZHAO

Chongqing Key Laboratory of Environmental Materials & Remediation Technologies, Chongqing University of Arts and Sciences, Chongqing-402160, P.R. China

**crossref** <http://dx.doi.org/10.5755/j01.ms.25.4.20603>

Received 18 April 2018; accepted 16 July 2018

Enhancing crystallization ability is a fundamental challenges in Poly(L-lactic acid) (PLLA) industry, therefore, the goal of this work was to synthesis a new organic nucleating agent *N, N'*-adipic bis(4-phenylbutyric acid) dihydrazide (APAD), and investigate its effect on non-isothermal crystallization, isothermal crystallization, melting behavior, thermal stability, and optical property of PLLA. Non-isothermal melt crystallization results showed that APAD acted as more effective nucleating and accelerating agent for the crystallization of PLLA, as a result, upon cooling at 1 °C/min, PLLA/0.5 %APAD had the highest onset crystallization temperature 136.4 °C and the crystallization peak temperature 132.0 °C, as well as the largest non-isothermal crystallization enthalpy 48.1 J/g. However, with increasing of APAD concentration from 0.5 wt.% to 3 wt.%, the crystallization peak shifted to the lower temperature. In contrast, for the non-isothermal cold crystallization process, the effect of APAD concentration on the crystallization behavior of PLLA was negligible. Additionally, the non-isothermal crystallization process was also depended on the cooling rates and the final melting temperature. In isothermal crystallization section, to compare with the primary PLLA, the crystallization half-time of PLLA/APAD could decrease from 254.3 s to the minimum value 29.4 s, with 0.5 wt.% APAD contents at 125 °C. Melting behavior of PLLA/APAD samples under different conditions further confirmed the heterogeneous nucleation effect of APAD for PLLA, and the appearance of the double melting peaks was attributed to the melting-recrystallization. Finally, the addition of APAD decreased the thermal stability to some extent, although APAD could not change the thermal decomposition profile of PLLA. And a drop of PLLA/APAD samples in light transmittance resulted from the double influence of the enhancement of crystallization and the opaqueness of APAD.

**Keywords:** Poly(L-lactic acid), heterogeneous nucleating agent, crystallization behavior, melting behavior, thermal stability.

### 1. INTRODUCTION

Among biodegradable polymers, Poly(L-lactic acid) (PLLA) is the most promising bio-based polymer to replace petroleum-based polymers, which have resulted in serious environmental pollution. It is the excellent biocompatibility, processability and biodegradability of PLLA that lead to a wider application potential in many fields such as food packaging [1–3], toy [4], medical materials [5, 6], agricultural [7], etc. For examples, a PLLA nanofiber membranes containing bovine lactoferrin was prepared using electrospun technology, the relevant measurements showed that the PLLA membranes exhibited no cytotoxicity on human skin fibroblasts and even promoted cell proliferation after short exposure periods. Additionally, the PLLA membranes also showed excellent antifungal activity against *Aspergillus nidulans*. Overall, the bovine lactoferrin-PLLA nanofiber membranes presents a powerful application potential in antifungal dressings [8]. Fu and his colleagues [9] developed the optical fibers based on PLLA with high mechanical flexibility and optical transparency, and PLLA fibers as a tool for intracranial light delivery and detection could realize deep brain fluorescence sensing and optogenetic interrogation in vivo.

However, the glass transition temperature of the amorphous PLLA is about 60 °C [10], which can not meet the using requirements of plastic products including disposable tableware, electronics enclosures and automotive interior parts [11]. For PLLA as a semi-crystalline polymer, enhancing the crystallinity of PLLA is one of the most effective way to improve its heat resistance. A ordered structure can restrict the movement of chain segments, resulting in a higher heat deformation temperature. Thereby improving the crystallization rate of PLLA in the manufacturing process has important guiding significance for theoretical research and practical application. The introduction of a nucleating agent into PLLA have been proved to be a good and cost-effective way for accelerating the crystallization process [10], resulting from that a nucleating agent can lower the surface free energy barrier to nucleation and initiate crystallization at a higher temperature zone in cooling [12]. Upon to now, a great deal of compounds with inorganic structures, organic structures, or macromolecular structures have been devoted to be as heterogenous nucleating agents for PLLA. Although inorganic nucleating agents such as talc [13], montmorilloite [14], zinc citrate [15], and macromolecular nucleating agents like nanocrystalline cellulose [16] exhibited advanced nucleation effect for PLLA, they need chemical modification to enhance their compatibility with PLLA, what is worse, the chemical modification may weaken the nucleation effect [17]. Thus,

\* Corresponding author. Tel.: +86-23-61162815; fax: +86-23-61162725. E-mail address: [caiyh651@aliyun.com](mailto:caiyh651@aliyun.com) (Y. Cai)

organic nucleating agents have attracted increasing attention in recent years because of their better compatibility [18] and remarkable nucleation ability, which was evaluated under the same conditions [19, 20]. For instance, the half-time of crystallization of PLLA could decrease into below 3 min after the addition of the adipic dihydrazides derivative during isothermal crystallization at 105 °C [21]. The other typical organic nucleating agents include benzoyl hydrazine derivatives [22, 23], oxamide derivatives [24, 25], myo-inositol [26, 27], 1H-benzotriazole derivatives [28, 29], etc.

Although more and more organic compounds could serve as nucleating agents for PLLA, the category and number of organic nucleating agents are very insufficient comparing to inorganic nucleating agents, even leading to undefined nucleation mechanism. Therefore, developing more novel organic nucleating agents is very necessary to PLLA scientific research and industry. Through structure analysis of the most organic nucleating agents for PLLA, it is found that the amide group could significantly increase the crystallization rate of PLLA [30]. Moreover, the rigidity of benzene and the flexibility of moderate alkyl are also necessary to bind the PLLA molecular chain. Thus, this work firstly synthesis a new organic nucleating agent *N, N'*-adipic bis(4-phenylbutyric acid) dihydrazide with amide group, benzene, and alkyl (APAD), and then its focus is to investigate its influence on non-isothermal and isothermal crystallization behavior of PLLA, as well as other physical properties including thermal stability and light transmittance.

## 2. EXPERIMENTAL

### 2.1. Materials

The PLLA (Trade name 2002D,  $M_n = 1.95 \times 10^5$ , a D-lactide content of 4.25 wt.%) used in this work was obtained from Nature Works LLC, USA. *N, N'*-adipic bis(4-phenylbutyric acid) dihydrazide (APAD) was synthesized in our laboratory with the chemical structure as shown in Fig. 1, (Characterization data: IR(KBr)  $\nu$ : 3454.6, 3213.3, 3029, 2936.9, 2860.8, 1651.1, 1596.2, 1484.4, 1450.9, 1411.9, 1248.2, 1194.3, 1152.2, 1028.9, 930.6, 744.9, 697.2  $\text{cm}^{-1}$ ;  $^1\text{H}$  NMR ( $d_6$ -DMSO, 400 MHz)  $\delta$ : ppm; 9.66 (s, 1H, NH), 9.65 (s, 1H, NH), 7.16 ~ 7.30 (m, 5H, Ar), 2.56 ~ 2.60 (t,  $J = 7.6$  Hz, 4H,  $\text{CH}_2$ ), 2.11 ~ 2.14 (t,  $J = 7.6$  Hz, 2H,  $\text{CH}_2$ ), 1.78 ~ 1.82 (t,  $J = 7.6$  Hz, 2H,  $\text{CH}_2$ ), 1.52 (s, 2H,  $\text{CH}_2$ )).

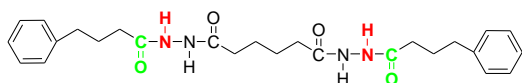


Fig. 1. Structure of APAD

### 2.2. Preparation of PLLA/APAD samples

All mixtures of PLLA and APAD (0.5, 1, 2, 3 wt.%) were dried overnight at 40 °C under vacuum to remove residual water. Subsequently, the melt-blending of each mixture was performed on a counter-rotating mixer (Harbin Hapro Electric Technology Co., Ltd., China) operated at 190 °C and the rotation speed of 32 rpm for 7 min, as well as 64 rpm for 5 min. The resulting product

was hot pressed at 190 °C under 20 MPa for 7 min to prepare a sheet, and then this sheet was cooled by being further pressed at room temperature under 20 MPa for 10 min.

## 2.3. Characterization and testing

The molecular structure of APAD was determined via  $^1\text{H}$  nuclear magnetic resonance spectrometer (AVANCE II 400MHz, Bruker Corporation, Switzerland) and infrared spectrometer (Nicolet iS50, Thermo Fisher Scientific, USA). The non-isothermal crystallization and melting behavior experiments were performed on a differential scanning calorimeter (Q2000, TA instrument, USA), operating under nitrogen atmosphere of 50 mL/min; additionally, the temperature and heat flow at different heating rates need to be calibrated using an indium standard before testing. The isothermal crystallization process of PLLA and PLLA/APAD samples were recorded using an optical depolarizer (GJY-III, Shanghai Donghua Kaili Technology of New Material Co., Ltd, China) in the region from 105 to 130 °C, and the half-time of the overall crystallization  $t_{1/2}$  was obtained from the corresponding isothermal crystallization curve. A thermogravimetric analysis (Q500, TA instrument, USA) was used to measure the thermal stability of the primary PLLA and PLLA/APAD samples under air flow in the region from room temperature to 650 °C, and the flow rate of air was 60 mL/min. The light transmittance of the primary PLLA and PLLA/APAD samples were directly tested by a light transmittance meter (DR82, Guanzhou Donru Electronic Technology Co., Ltd, China).

## 3. RESULTS AND DISCUSSION

### 3.1. Non-isothermal crystallization

The role of APAD in crystallization process of PLLA was examined through a comparative study of the non-isothermal crystallization behavior of the primary PLLA and PLLA/APAD samples. Fig. 2 shows the DSC curves of non-isothermal crystallization from 190 °C at a cooling rate of 1 °C/min. It is observed clearly that the primary PLLA does almost not have visible crystallization in cooling, implying that it is very difficult for the primary PLLA to form the crystal because of chain stiffness and lack of nucleators [31], this poor nucleation ability of the primary PLLA were also confirmed by other relevant studies [20, 32]. In contrast, with addition of APAD, the non-isothermal crystallization peaks with different height and location appear in DSC cooling curves, which indicates that APAD as a heterogenous nucleating agent can promote the crystallization of PLLA in cooling. This result also illustrates that, in comparison to the crystal growth rate, the nucleation rate is a rate-determining step for the melt crystallization process. Among these PLLA/APAD samples, PLLA/0.5 %APAD exhibits the highest onset crystallization temperature of 136.4 °C and crystallization peak temperature of 132.0 °C, as well as the largest non-isothermal crystallization enthalpy of 48.1 J/g, indicating that the enhancement of 0.5 wt.% APAD on the crystallization of PLLA is the best. On the other hand, under the same circumstance, the higher onset

crystallization temperature and crystallization peak temperature, as well as the larger non-isothermal crystallization enthalpy of PLLA/APAD system further confirm the more powerful accelerating ability of APAD for PLLA crystallization comparing with other systems such as PLLA/BASD [11], PLLA/NA [33], PLLA/MCB [34]. Additionally, with increasing of APAD concentration, the crystallization peak shifts to the lower temperature, and the value of the non-isothermal crystallization enthalpy also becomes smaller. This negative effect might be because of an inhibition effect of excessive APAD for melt crystallization of PLLA to some extent.

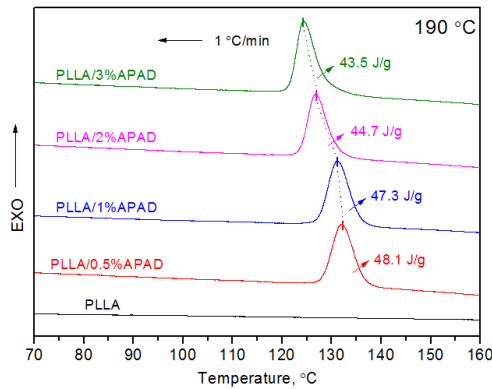


**Fig. 2.** DSC curves of the primary PLLA and PLLA/APAD samples cooling at 1 °C/min

However, for non-isothermal cold crystallization process, the DSC heating curves profiles of all PLLA/APAD samples are thoroughly similar, additionally the values of crystallization peak temperature and non-isothermal crystallization enthalpy of all PLLA/APAD samples only exhibit a slight difference (see Fig. 3). Overall, the effect of APAD concentration on the crystallization behavior of PLLA is negligible. In low temperature zone, PLLA has very fast nucleation rate resulting from the existence of a heterogenous nucleating agent APAD and nucleus of PLLA itself, resulting in that the crystal growth rate is a rate-determining step.

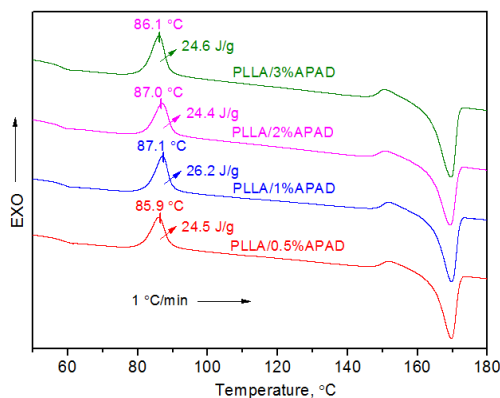


**Fig. 3.** DSC curves of all PLLA/APAD samples from 50 °C at a heating rate of 1 °C/min

On the other hand, the crystal growth rate depends on the motility of molecular chain segment and temperature, a same heating rate causes PLLA/APAD sample to go through the same temperature variation. Under these

circumstances, all PLLA/APAD samples present the rather similar crystallization process. Although PLLA/0.5 %APAD has the best crystallization ability upon cooling at 1 °C/min, the faster cooling rate is often required during manufacturing. Thus, it is very necessary to investigate the crystallization process of the PLLA/0.5 %APAD sample under the faster cooling rates. The DSC cooling curves of the PLLA/0.5 %APAD at different rates are shown in Fig. 4.

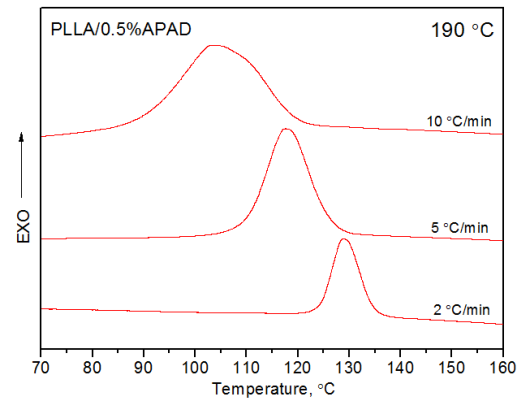


**Fig. 4.** DSC cooling curves of the PLLA/0.5%APAD at different rates

Considering the poor crystallization ability of the primary PLLA showed aforementioned non-isothermal crystallization process in cooling at 1 °C/min, the non-isothermal crystallization trace of PLLA/0.5 %APAD can be still detected upon the faster cooling rates, which further reflects the advanced nucleation capability of APAD for PLLA. However, it is found that the crystallization peak shifts to lower temperature and becomes wider with increasing of cooling rate, indicating that a higher cooling rate can weaken the crystallization promoting effect of the nucleating agent for PLLA, and form more imperfect crystals. Similar results can be also found in other PLLA systems [35–37]. The effect of heating rate on cold crystallization of PLLA was further investigated and shown in Fig. 5. Similarly, a wider cold crystallization peak appears with increasing of heating rate in heating. However, the cold crystallization peak shifts to the higher temperature because of thermal inertia.

Additionally, for organic nucleating agent, the solubility in PLLA matrix is a crucial factor for improving crystallization, because the compatibility and undissolved organic nucleating agent are directly related to the solubility. Whereas the solubility of organic nucleating agent in PLLA matrix is determined by the final melt-blending temperature. Therefore, the effect of the final melt-blending temperature on the crystallization of PLLA was further studied using DSC. Fig. 6 is the non-isothermal crystallization curves of PLLA/APAD samples from the different melt-blending temperatures at a cooling rate of 1 °C/min. When the final melt-blending temperature is 180 °C or 200 °C, PLLA containing the same APAD concentration has the similar non-isothermal crystallization DSC curves, which are different from the non-isothermal melt crystallization DSC curves from the 190 °C (see Fig. 2).

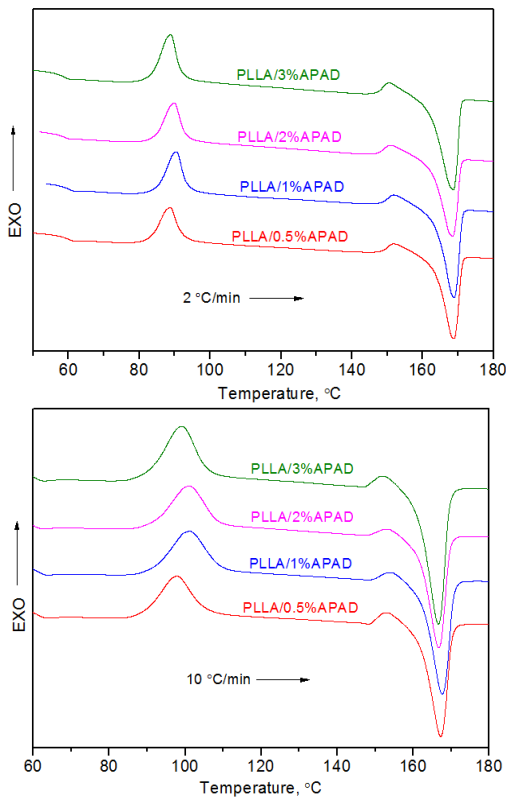


Fig. 5. DSC heating curves of the PLLA/APAD samples at different rates

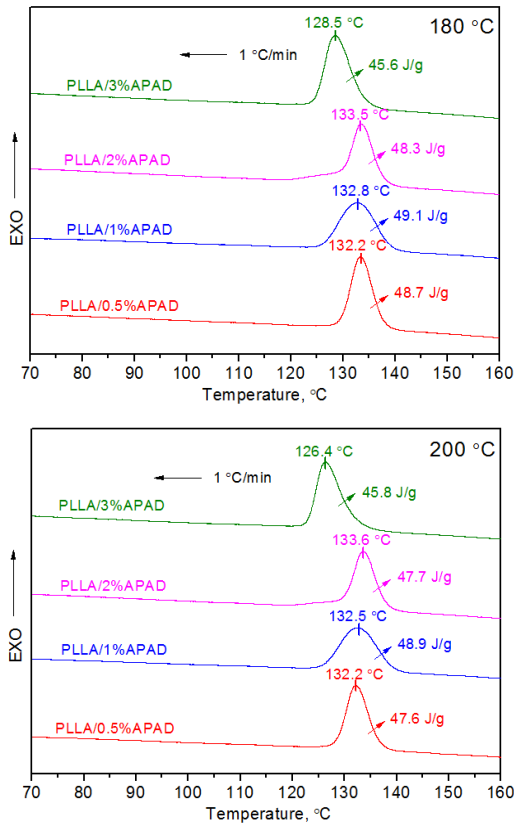


Fig. 6. Non-isothermal crystallization curves of PLLA/APAD samples from the different melt-blending temperatures

That is, with increasing of APAD concentration, the crystallization enthalpy and crystallization peak temperature firstly increase, then decrease, and

PLLA/1 %APAD sample has the largest non-isothermal crystallization enthalpy, however, the highest crystallization peak temperature appears on PLLA/2 %APAD sample.

The probable reason is that the solubility of APAD in PLLA matrix is lower, more undissolved APAD become nuclei for the dissolved APAD and for PLLA in cooling, resulting in higher nucleation density, meantime, the dissolved APAD can lead toward excellent compatibility. This result also indicates that 180 °C is the optimal melt-blending temperature in this study.

In addition, upon the addition of the same APAD concentration, comparing to the final melt-blending temperature of 190 °C or 200 °C, the larger crystallization enthalpy and higher crystallization temperature occur when the final melt-blending temperature is 180 °C.

### 3.2. Isothermal crystallization

For semi-crystalline polymer, the isothermal crystallization is an important part of crystallization behavior. Fig. 7 shows the half-time of crystallization ( $t_{1/2}$ ) as a function of crystallization temperature ( $T_c$ ) for the primary PLLA and PLLA/APAD samples. It is found that overall the  $t_{1/2}$  of the primary PLLA firstly decreases with increasing of crystallization temperature, then increases. This trend depends on the effect of crystallization temperature on the motility of macromolecule segment [38], and the primary PLLA has the minimum  $t_{1/2}$  value of 139.3 s at 120 °C. However, for PLLA/APAD samples, the influences of  $T_c$  and APAD concentration on  $t_{1/2}$  are concluded into two types. When the  $T_c$  is 105 °C ~ 110 °C, an increase of APAD concentration leads to a drop in  $t_{1/2}$ , the reason is that the existence of more APAD can produce a higher nucleation density in PLLA matrix, meantime, the temperature range of 105 °C ~ 110 °C can cause the macromolecule segment to possess excellent active ability, which results in a decrease of  $t_{1/2}$ . In contrast, it is observed from Fig. 7 that more APAD loading gives rise to an increase of  $t_{1/2}$  if the  $T_c$  is further increased, because the synergistic effect of excessive macromolecule segment activity and impediment effect of more APAD in PLLA matrix must restrict the formation of crystal. To compare with the primary PLLA,  $t_{1/2}$  decreases from 254.3 s to the minimum value 29.4 s, with 0.5 wt.% APAD at 125 °C.

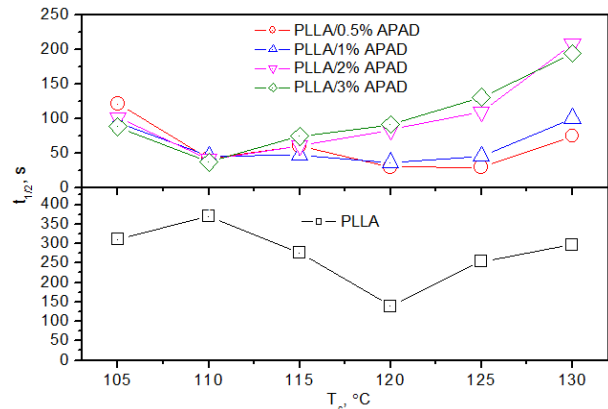
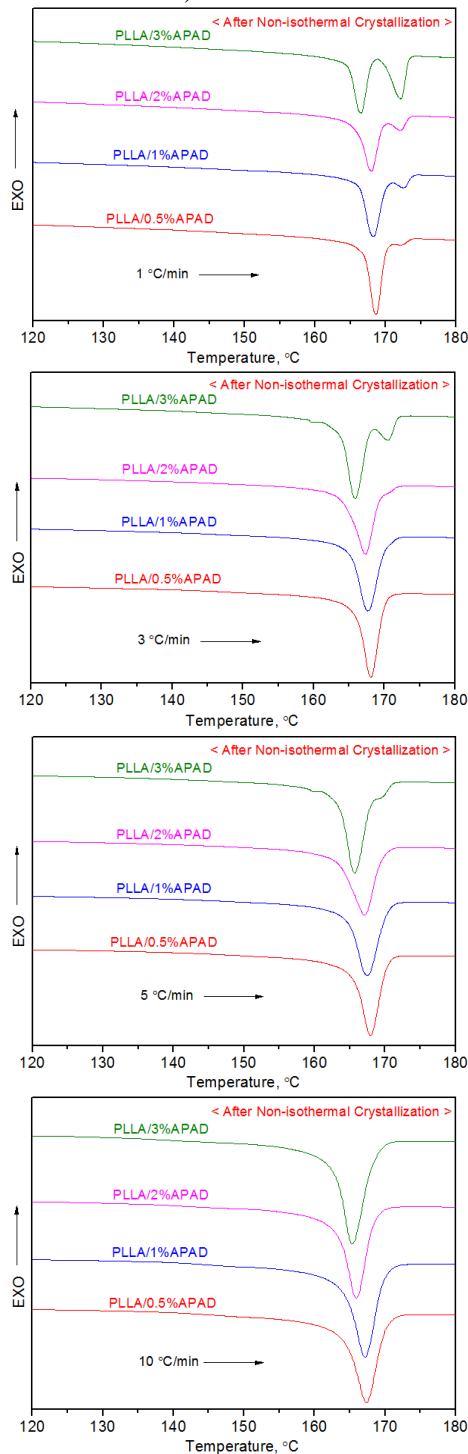


Fig. 7. The  $t_{1/2}$  for PLLA/APAD with different APAD concentration plotted as a function of  $T_c$

### 3.3. Melting behavior

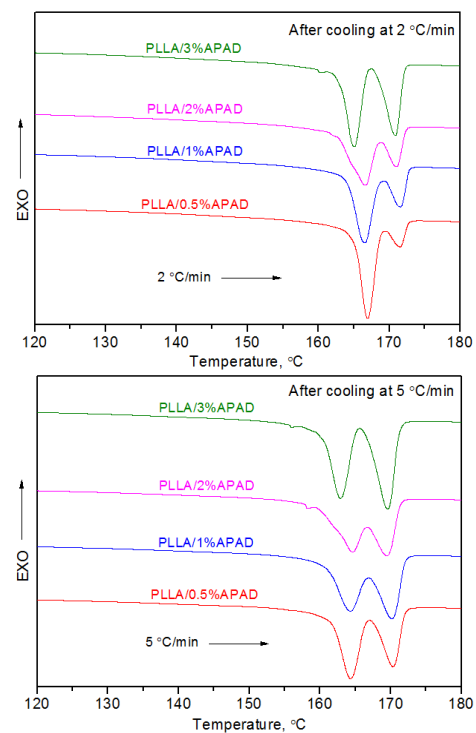
Melting behavior of semi-crystalline polymer during the second heating scan is related with the crystallinity and perfection of crystals. Investigating the melting behavior of PLLA/APAD samples under different conditions can further reflect the role of APAD in crystallization process of PLLA. Fig. 8 presents the melting curves of PLLA containing various APAD concentrations at different heating rates after non-isothermal crystallization (Cooling at 1 °C/min from 190 °C).



**Fig. 8.** DSC heating curves of PLLA/APAD at a different rate after non-isothermal crystallization cooling at 1 °C/min

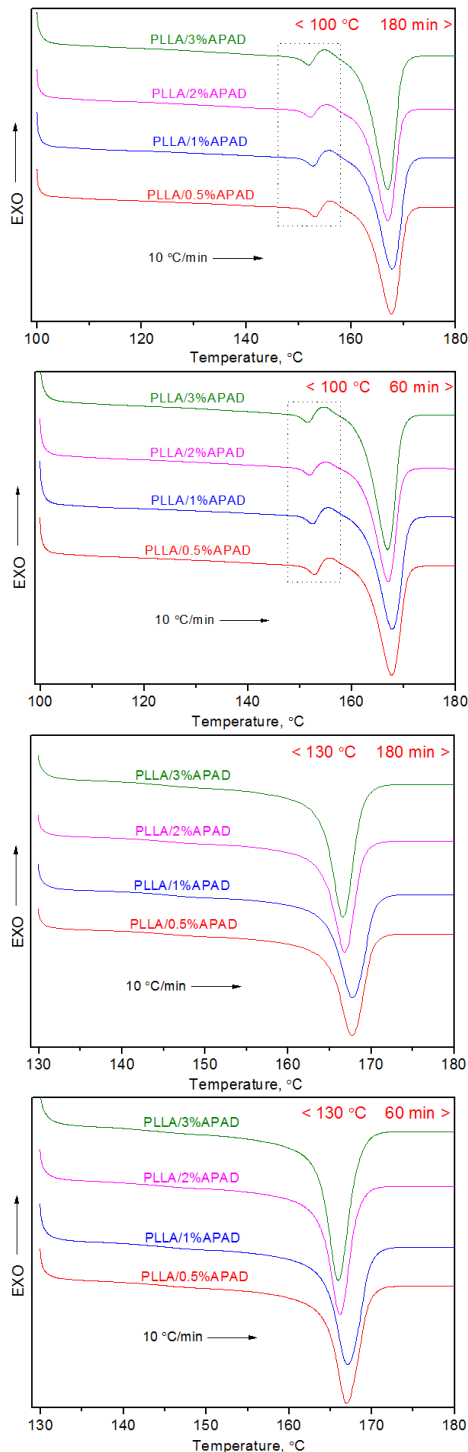
As shown in Fig. 8, the existence of double melting peaks is very clear (heating at 1 °C/min), indicating that, according to melting-recrystallization mechanism [39, 40], the recrystallization behavior occurs rapidly after melting of the primary crystallites formed in cooling. Furthermore, for PLLA containing a higher APAD loading, there is more visible high-temperature melting peak, resulting from that a more un-nucleated APAD in PLLA matrix can cause the melted crystals to grow into more new crystals in heating [41]. However, with increasing of heating rate ranging from 3 °C/min to 10 °C/min, the double melting peaks gradually degenerate into the single melting peak, this is because there is not enough time to form the crystals under a faster heating rate, exhibiting a competitive relationship between heating rate and APAD for improving crystallization of PLLA. On the other hand, this result further confirms that the double-melting peaks of PLLA/APAD samples result from melting-recrystallization rather than crystal polymorphism.

Fig. 9 presents the melting behavior of PLLA/APAD samples at different heating rates that corresponded to the rates of non-isothermal crystallization at different cooling rates. It is noted that, for the same PLLA/APAD sample, the peak area ratio of low-temperature melting peak and high-temperature melting peak decreases evidently with increasing of rate, even the high-temperature melting peak, in comparison to the low-temperature melting peak, has the larger peak area when the rate is 5 °C/min, this is due to the more dramatic influence of rate on crystallization of PLLA comparing to the crystallization accelerator APAD. However, under the circumstance with the same rate, the effect of APAD concentration on melting behavior of PLLA is similar.



**Fig. 9.** Melting behavior of PLLA/APAD samples at different heating rates corresponding to the rate of non-isothermal crystallization at different cooling rates

As aforementioned, the isothermal crystallization behavior of PLLA depends upon significantly the crystallization temperature. Here, the melting behavior after isothermal crystallization at different crystallization temperatures (high temperature: 130 °C, low temperature: 100 °C) was further studied by DSC (see Fig. 10).



**Fig. 10.** Melting behavior of PLLA/APAD samples after isothermal crystallization at 100 °C and 130 °C for different crystallization time

When the crystallization temperature is 100 °C, all PLLA/APAD samples have double melting peaks, moreover, the double melting peaks are irrelevant with the various crystallization time from 60 min to 180 min,

implying that it is very difficult to thoroughly complete crystallization in low temperature zone because of poor macromolecule segment activity. In contrast, upon the crystallization temperature of 130 °C, the existence of APAD and excellent macromolecule segment activity ensure high nuclear rate and crystal growth rate, resulting in the appearance of the single melting peak after isothermal crystallization for 60 ~ 180 min which ensures complete crystallization. This result also evidences the crystallization temperature dependence of melting behavior of PLLA.

### 3.4. Thermal stability and optical properties

In industry, thermal stability is an important index which determines the working or using temperature of polymers. Fig. 11 is the TGA thermograms profiles for the primary PLLA and PLLA/APAD samples at a heating rate of 5 °C/min from room temperature to 650 °C. It is a fact that the addition of APAD can not change the thermal decomposition profile of PLLA, both the primary PLLA and PLLA/APAD samples only exhibit one thermal decomposition stage. However, the onset decomposition temperature ( $T_o$ ) of modified PLLA depends on the APAD concentration, and the  $T_o$  of the primary PLLA, PLLA/0.5 %APAD, PLLA/1 %APAD, PLLA/2 %APAD, and PLLA/3 %APAD are observed at 341.3, 325.8, 321.4, 319.1, and 333.6 °C, respectively. Through the analysis of  $T_o$  data, it is found that the addition of APAD more or less decreases the thermal stability. And the maximal weight loss observed between 300 to 370 °C can be ascribed to the chain scissions and loss of ester groups [42, 43]. Additionally, when the APAD concentration is 0.5 ~ 2 wt.%, the  $T_o$  decreases with increasing of APAD concentration because of low decomposition temperature of APAD itself, but the  $T_o$  of PLLA/3 %APAD is higher than that of other PLLA/APAD samples, the increase in  $T_o$  is thought to be due to winding effect of excessive APAD in PLLA matrix.

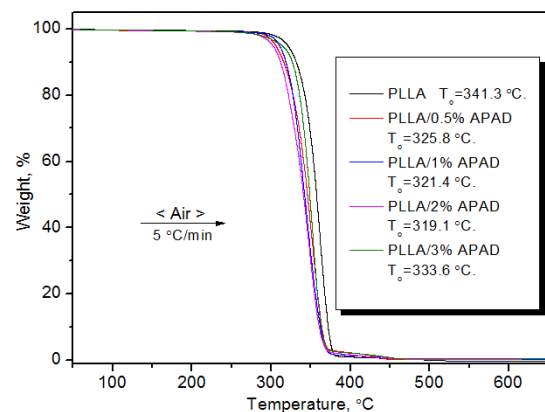


**Fig. 11.** TGA profiles for the primary PLLA and PLLA/APAD samples under air

Additionally, the light transmittance of the primary PLLA and PLLA/APAD samples was further evaluated. As seen in Fig. 12, the introduction of APAD leads to an extreme decrease in the light transmittance of PLLA, even the light transmittance is almost zero when the APAD content is larger than 2 wt.%, still resulting from the enhancement of crystallization, and the opaqueness of

APAD itself. However, it is noted that the light transmittance of PLLA/0.5 %APAD sample is higher than 50 %, meaning that the PLLA/0.5 %APAD sample has a good performance in crystallization and optical property.

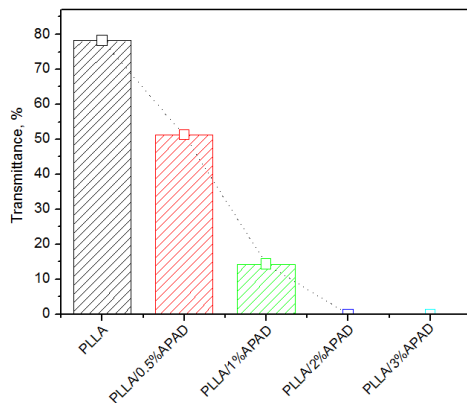


Fig. 12. Light transmittance of the primary PLLA and PLLA/APAD samples

#### 4. CONCLUSIONS

In this work, APAD was synthesized to investigate its influence on non-isothermal crystallization, isothermal crystallization, melting behavior, thermal stability and optical property. The relevant results indicated that APAD could significantly accelerate the crystallization of PLLA in cooling, and 0.5 wt.% APAD had the best crystallization nucleation ability for PLLA *via* a comparison on the onset crystallization temperature, the crystallization peak temperature and the non-isothermal crystallization enthalpy, and the result of isothermal crystallization also showed that PLLA/0.5 %APAD had the smallest  $t_{1/2}$  29.4 s at 125 °C. In addition, the non-isothermal crystallization process of PLLA/APAD samples remarkably affected by cooling rate and the final melting temperature, as a result, 180 °C was evaluated as the optimal melt-blending temperature for PLLA/APAD. The melting behaviors after non-isothermal crystallization and isothermal crystallization reflected the crystallization accelerating effect of APAD for PLLA, and the double melting peaks occurred under different conditions resulted from the melting-recrystallization. A comparison study on thermal stability of the primary PLLA and PLLA/APAD samples showed that the introduction of APAD decreased the onset thermal decomposition temperature, but the thermal stability of PLLA/APAD samples was also affected by APAD concentration. However, the light transmittance significantly decreased with increasing of APAD concentration.

#### Acknowledgements

This work was supported by National Natural Science Foundation of China (project number 51403027), Foundation of Chongqing Municipal Science and Technology Commission (project number cstc2015jcyjBX0123 and cstc2017shmsA20021), Scientific and Technological Research Program of Chongqing Municipal Education Commission (project number KJ1601101), Innovation Team Project of

Chongqing Municipal Education Commission (project number CXTDX201601037), and Natural Science Foundation Project of Yongchuan District (project number Ycstc, 2017nc4002).

#### REFERENCES

1. Davachi, S.M., Bakhtiari, S., Pouresmaeel-Selakjani, P., Mohammadi-Rovshandeh, J., Kaffashi, B., Davoodi, S., Yousefi, A. Investigating the Effect of Treated Rice Straw in PLLA/Starch Composite: Mechanical, Thermal, Rheological, and Morphological Study *Advances in Polymer Technology* 37 (1) 2018: pp. 21634.1–21634. 12. <http://doi.org/10.1002/adv.21634>
2. Wang, L., Lee, R.E., Wang, G.L., Chu, R.K.M., Zhao, J.C., Park, C.B. Use of Stereocomplex Crystallites for Fully-biobased Microcellular Low-density Poly(lactic acid) Foams for Green Packaging *Chemical Engineering Journal* 327 2017: pp.1151–1162. <http://doi.org/10.1016/j.cej.2017.07.024>
3. Mohammadi-Rovshandeh, J., Pouresmaeel-Selakjani, P., Davachi, S.M., Kaffashi, B., Hassani, A., Bahmehl, A. Effect of Lignin Removal on Mechanical, Thermal, and Morphological Properties of Polylactide/Starch/Rice Husk Blend Used in Food Packaging *Journal of Applied Polymer Science* 131 (22) 2014: pp. 41095.1–41095.8. <http://doi.org/10.1002/APP.41095>
4. Garcia, A.M., Garcia, A.I., Cabezas, M.L., Reche, A.S. Study of the Influence of the Almond Variety in the Properties of Injected Parts with Biodegradable Almond Shell Based Masterbatches *Waste and Biomass Valorization* 6 (3) 2015: pp. 363–370. <http://doi.org/10.1007/s12649-015-9351-x>
5. Pan, Y.H., Wang, H.T., Wu, T.L., Fan, K.H., Huang, H.M., Chang, W.J. Fabrication of Fe<sub>3</sub>O<sub>4</sub>/PLLA Composites for Use in Bone Tissue Engineering *Polymer Composites* 38 (12) 2017: pp. 2881–2888. <http://doi.org/10.1002/pc.23890>
6. Santos, D., Silva, D.M., Gomes, P.S., Fernandes, M.H., Santos, J.D., Sencadas, V. Multifunctional PLLA-Ceramic Fiber Membranes Applications for Bone Regeneration *Journal of Colloid and Interface Science* 504 2017: pp. 101–110. <http://doi.org/10.1016/j.jcis.2017.05.032>
7. Li, Y., Han, C.Y., Yu, Y.C., Xiao, L.G., Shao, Y. Isothermal and Nonisothermal Cold Crystallization Kinetics of Poly(L-lactide)/Functionalized Eggshell Powder Composites *Journal of Thermal Analysis and Calorimetry* 131 (3) 2018: pp. 2213–2233. <http://doi.org/10.1007/s10973-017-6783-5>
8. Machado, R., da Costa, A., Silva, D.M., Gomes, A.C., Casal, M., Sencadas, V. Antibacterial and Antifungal Activity of Poly(Lactic acid)-Bovine Lactoferrin Nanofiber Membranes *Macromolecular Bioscience* 18 (3) 2018: pp. 1700324.1–1700324.10. <http://doi.org/10.1002/mabi.201700324>
9. Fu, R.X., Luo, W.H., Nazempour, R., Tan, D.X., Ding, H., Zhang, K.Y., Yin, L., Guan, J.S., Sheng, X. Implantable and Biodegradable Poly(L-lactic acid) Fibers for Optical Neural Interfaces *Advanced Optical Materials* 6 (3) 2018: pp. 1700941. <http://doi.org/10.1002/adom.201700941>
10. Luo, C.Y., Yang, M.R., Xiao, W., Yang, J.J., Wang, Y., Chen, W.X., Han, X. Relationship Between the Crystallization Behavior of Poly(ethylene glycol) and

- Stereocomplex Crystallization of Poly(L-lactic acid)/Poly(D-lactic acid) *Polymer International* 67 2018: pp. 313–321.  
<http://doi.org/10.1002/pi.5506>
11. **Fan, Y.Q., Yu, Z.Y., Cai, Y.H., Hu, D.D., Yan, S.F., Chen, X.S., Yin, J.B.** Crystallization Behavior and Crystallite Morphology Control of Poly(L-lactic acid) Through *N, N'*-Bis(benzoyl)sebacic Acid Dihydrazide *Polymer International* 62 2013: pp. 647–657.  
<http://doi.org/10.1002/pi.4342>
  12. **Saad, G.R., Elsayy, M.A., Aziz, M.S.A.** Nonisothermal Crystallization Behavior and Molecular Dynamics of Poly(lactic acid) Plasticized with Jojoba Oil *Journal of Thermal Analysis and Calorimetry* 128 (1) 2017: pp. 211–223.  
<http://doi.org/10.1007/s10973-016-5910-z>
  13. **Cipriano, T.F., da Silva, A.L.N., da Silva, A.H.M.D.F.T., de Sousa, A.M.F., da Silva, G.M., Rocha, M.G.** Thermal, Rheological and Morphological Properties of Poly(lactic acid)(PLA) and Talc Composites *Polimeros-Ciencia E Tecnologia* 24 (3) 2014: pp. 276–282.  
<http://doi.org/10.4322/polimeros.2014.067>
  14. **Wu, T., Tong, Y.R., Qiu, F., Yuan, D., Zhang, G.Z., Qu, J.P.** Morphology, Rheology Property, and Crystallization Behavior of PLLA/OMMT Nanocomposites Prepared by an Innovative Eccentric Rotor Extruder *Polymers for Advanced Technologies* 2018: pp. 41–51.  
<http://doi.org/10.1002/pat.4087>
  15. **Teranishi, S., Kusumi, R., Kimura, F., Kimura, T., Aburaya, K., Maeyama, M.** Biaxial Magnetic Orientation of Zinc Citrate as Nucleating Agent of Poly(L-lactic acid) *Chemistry Letters* 46 (6) 2017: pp. 830–832.  
<http://doi.org/10.1246/cl.170092>
  16. **Feng, Y.Q., Lv, P., Jiang, L., Ma, P.M., Chen, M.Q., Dong, W.F., Chen, Y.J.** Enhanced Crystallization Kinetics of Symmetric Poly(L-lactide)/Poly(D-lactide) Stereocomplex in the Presence of Nanocrystalline Cellulose *Polymer Degradation and Stability* 146 2017: pp. 113–120.  
<http://doi.org/10.1016/j.polymerdegradstab.2017.10.002>
  17. **Liang, Y.Y., Xu, J.Z., Liu, X.Y., Zhong, G.J., Li, Z.M.** Role of Surface Chemical Groups on Carbon Nanotubes in Nucleation for Polymer Crystallization: Interfacial Interaction and Steric Effect *Polymer* 54 (23) 2013: pp. 6479–6488.  
<http://doi.org/10.1016/j.polymer.2013.09.027>
  18. **Jiang, L., Shen, T.F., Xu, P.W., Zhao, X.Y., Li, X.J., Dong, W.F., Ma, P.M., Chen, M.Q.** Crystallization Modification of Poly(lactide) by Using Nucleating Agents and Stereocomplexation *E-Polymers* 16 (1) 2016: pp. 1–13.  
<http://doi.org/10.1515/epoly-2015-0179>
  19. **Zhang, X.Q., Meng, L.Y., Li, G., Liang, N.N., Zhang, J., Zhu, Z.G., Wang, R.** Effect of Nucleating Agents on the Crystallization Behavior and Heat Resistance of Poly(L-lactide) *Journal of Applied Polymer Science* 133 2016: pp. 42999.1–42999.7.  
<http://doi.org/10.1002/app.42999>
  20. **Feng, Y.Q., Ma, P.M., Xu, P.W., Wang, R.Y., Dong, W.F., Chen, M.Q., Joziassé, C.** The Crystallization Behavior of Poly(lactic acid) with Sifferent Types of Nucleating Agents *International Journal of Biological Macromolecules* 106 2018: pp. 955–962.  
<http://doi.org/10.1016/j.ijbiomac.2017.08.095>
  21. **Qi, Z.F., Yang, Y., Xiong, Z., Deng, J., Zhang, R.Y., Zhu, J.** Effect of Aliphatic Diacyl Adipic Dihydrazides on the Crystallization of Poly(lactic acid) *Journal of Applied Polymer Science* 132 2015: pp. 42028.1–42028.8  
<http://doi.org/10.1002/app.42028>
  22. **Kawamoto, N., Sakai, A., Horikoshi, T., Urushihara, T., Tobita, E.** Physical and Mechanical Properties of Poly(L-lactic acid) Nucleated by Dibenzoylhydrazide *Journal of Applied Polymer Science* 103 (1) 2007: pp. 244–250.  
<http://doi.org/10.1002/app.25185>
  23. **Yamato, M., Kudo, Y., Takahashi, K., Watanabe, K., Kawamoto, N.** Magnetic Alignment of Poly(L-lactic acid) Containing a Nucleating Agent *Chemistry Letters* 40 (7) 2011: pp. 765–767.  
<http://doi.org/10.1246/cl.2011.765>
  24. **Shen, T.F., Xu, Y.S., Cai, X.X., Ma, P.M., Dong, W.F., Chen, M.Q.** Enhanced Crystallization Kinetics of Poly(lactide) with Oxalamide Compounds as Nucleators: Effect of Space Length Between the Oxalamide Moieties *RSC Advances* 6 (54) 2016: pp. 48365–48374.  
<http://doi.org/10.1039/C6RA04050K>
  25. **Ma, P.M., Xu, Y.S., Wang, D.W., Dong, W.F., Chen, M.Q.** Rapid Crystallization of Poly(lactic acid) by Using Tailor-made Oxalamide Derivatives as Novel Soluble-type Nucleating Agents *Industrial & Engineering Chemistry Research* 53 (32) 2014: pp. 12888–12892.  
<http://doi.org/10.1021/ie502211j>
  26. **Tachibana, Y., Maeda, T., Ito, O., Maeda, Y., Kunioka, M.** Biobased *myo*-inositol as Nucleator and Stabilizer for Poly(lactic acid) *Polymer Degradation and Stability* 95 (8) 2010: pp. 1321–1329.  
<http://doi.org/10.1016/j.polymerdegradstab.2010.02.007>
  27. **Shi, H., Chen, X., Chen, W.K., Pang, S.J., Pan, L.S., Xu, N., Li, T.** Crystallization Behavior, Heat Resistance, and Mechanical Performances of PLLA/*myo*-inositol Blends *Journal of Applied Polymer Science* 134 (16) 2017: pp. 44732.1–44732.13.  
<http://doi.org/10.1002/app.44732>
  28. **Cai, Y.H., Tang, Y., Zhao, L.S.** Poly(L-lactic acid) with Organic Nucleating Agent *N, N, N'*-tris(1H-benzotriazole) Trimesinic Acid Acetylhydrazide: Crystallization and Melting Behavior *Journal of Applied Polymer Science* 132 (32) 2015: pp. 42402.1–42402.7.  
<http://doi.org/10.1002/app.42402>
  29. **Cai, Y.H., Zhao, L.S., Tang, Y.** Thermal Performance of a Blend System Based on Poly(L-lactic acid) and an Aliphatic Multiamide Derivative Derived from 1H-benzotriazole *Journal of Macromolecular Science, Part B Physics* 56 (1) 2017: pp. 64–73.  
<http://doi.org/10.1080/00222348.2016.1261594>
  30. **Wang, T., Yang, Y., Zhang, C., Tang, Z., Na, H., Zhu, J.** Effect of 1,3,5-Trialkyl-Benzenetricarboxylamide on the Crystallization of Poly(lactic acid) *Journal of Applied Polymer Science* 130 2013: pp. 1328–1336.  
<http://doi.org/10.1002/app.39308>
  31. **Saeldlou, S., Huneault, M.A., Li, H.B., Park, C.B.** Poly(lactic acid) Crystallization *Progress in Polymer Science* 37(12) 2012: pp.1657-1677.  
<http://doi.org/10.1016/j.progpolymsci.2012.07.005>
  32. **Shen, T.F., Ma, P.M., Yu, Q.Q., Dong, W.F., Chen, M.Q.** The Effect of Thermal History on the Fast Crystallization of Poly(L-lactide) with Soluble-type Nucleators and Shear Flow *Polymers* 8 2016: pp. 431.1–431.12.  
<http://doi.org/10.3390/polym8120431>
  33. **Cai, Y.H., Yan, S.F., Yin, J.B., Fan, Y.Q., Chen, X.S.** Crystallization Behavior of Biodegradable Poly(L-lactic acid)



Filled with a Powerful Nucleating Agent-*N, N'*-Bis(benzoyl) Suberic Acid Dihydrazide *Journal of Applied Polymer Science* 121 (3) 2011: pp. 1408–1416.  
<http://doi.org/10.1002/app.33633>

34. **Su, Z.Z., Li, Q.Y., Liu, Y.J., Guo, W.H., Wu, C.F.** The Nucleation Effect of Modified Carbon Black on Crystallization of Poly(lactic acid) *Polymer Engineering and Science* 50 2010: pp. 1658–1666.  
<http://doi.org/10.1002/pen.21621>
35. **Cai, Y.H., Zhao, L.S., Zhang, Y.H.** Role of *N, N'*-Bis(1H-benzotriazole) Adipic Acid Acethydrazide in Crystallization Nucleating Effect and Melting Behavior of Poly(L-lactic acid) *Journal of Polymer Research* 22 2015: pp. 246.1–246.9.  
<http://doi.org/10.1007/s10965-015-0887-z>
36. **Su, Z.Z., Guo, W.H., Liu, Y.J., Li, Q.Y., Wu, C.F.** Non-isothermal Crystallization Kinetics of Poly(lactic acid)/Modified Carbon Black Composite *Polymer Bulletin* 62 2009: pp. 629–642.  
<http://doi.org/10.1007/s00289-009-0047-x>
37. **Cai, Y.H., Zhao, L.S.** Thermal Behavior of Modified Poly(L-lactic acid): Effect of Aromatic Multiamides Derivative Based on 1H-benzotriazole *E-Polymers* 16 (4) 2016: pp. 303–311.  
<http://doi.org/10.1515/epoly-2016-0052>
38. **Li, X.X., Yin, J.B., Yu, Z.Y., Yan, S.F., Lu, X.C., Wang, Y.J., Cao, B., Chen, X.S.** Isothermal Crystallization Behavior of Poly(L-lactic acid)/Organo-montmorillonite Nanocomposites *Polymer Composites* 30 2009: pp. 1338–1344.  
<http://doi.org/10.1002/pc.20721>
39. **Yasuniwa, M., Satou, T.** Multiple Melting Behavior of Poly(butylene succinate).I. Thermal Analysis of Melt-Crystallized Samples *Journal of Polymer Science: Part B: Polymer Physics* 40 (21) 2002: pp. 2411–2420.  
<http://doi.org/10.1002/polb.10298>
40. **Cai, Y.H.** Nucleation, Melting Behaviour and Mechanical Properties of Poly(L-lactic acid) Affected by the Addition of *N, N'*-Bis(benzoyl) Suberic Acid Dihydrazide *South African Journal of Chemistry-Suid- Afrikaanse Tydskrif vir Chemie* 64 2011: pp. 115–119.
41. **Xin, C.Z., Zhang, H., Wang, Y.W., Yu, X.** Study on Multiple Melting Transformation and Cold-Crystallization Behaviors of PLA *Plastics Science and Technology* 45 (1) 2017: pp. 75–77 (In Chinese).
42. **Elsawy, M.A., Saad, G.R., Sayed, A.M.** Mechanical, Thermal, and Dielectric Properties of Poly(lactic acid)/Chitosan Nanocomposites *Polymer Engineering and Science* 56 (9) 2016: pp. 987–994.  
<http://doi.org/10.1002/pen.24328>
43. **Cai, Y.H., Zhao, L.S.** Non-isothermal Crystallization, Thermal Stability, and Mechanical Performances of Poly(L-lactic acid)/Barium Phenylphosphonate Systems *Open Chemistry* 15 2017: pp. 248–254.  
<http://doi.org/10.1515/chem-2017-0029>